PHYSICAL REVIEW C VOLUME 34, NUMBER 2 AUGUST 1986

Rapid Communications

The Rapid Communications section is intended for the accelerated publication of important new results. Manuscripts submitted to this section are given priority in handling in the editorial office and in production. A Rapid Communication may be no longer than 3½ printed pages and must be accompanied by an abstract. Page proofs are sent to authors, but, because of the rapid publication schedule, publication is not delayed for receipt of corrections unless requested by the author.

Expanding pion emitting source in Ar on Pb collisions

D. Beavis,* S. Y. Chu, S. Y. Fung, D. Keane, Y. M. Liu, G. VanDalen, and M. Vient
Department of Physics, University of California, Riverside, California 92521
(Received 12 May 1986)

We report results of a pion interferometry analysis for central collisions of 1.8 GeV/nucleon Ar on Pb at the Bevalac streamer chamber. The statistics are sufficient to allow a detailed study of the spatial structure of the pion emitting source. The dependence of the size of the source on the average magnitude of the momenta of the emitted pion pairs is consistent with the picture of an expanding pion source. There are also indications that the Ar nucleus is completely stopped by the Pb target in the most central collisions.

The study of the Hanbury-Brown Twiss effect[1] for like pions has already proven its usefulness in heavy ion collisions at currently available energies.[2-5] The size and the lifetime of the pion source and the phase coherence of the emitted pions can be determined. With increasing statistics, a more detailed analysis of the space-time structure of the interaction region can be made through multiplicity or energy cuts, measurements of different correlation functions, and use of different species of identical particles. We report results of such a pion interferometry analysis.

The data for this investigation come from a streamer chamber experiment at the Lawrence Berkeley Laboratory with a 1.8 GeV/nucleon Ar beam incident on a Pb_3O_4 target. The central collision trigger suppresses events corresponding to collisions of Ar on oxygen; we estimate that this component amounts to less than 5% of the present sample. The events selected by the trigger correspond, in a geometric picture, to central collisions on Pb with impact parameter ≤ 5 fm. Details of the trigger and the scanning procedure have been reported earlier.[3,4] After a kinematic selection ($p_{\rm lab} \geq 100$ MeV/c; see below), there are 3500 events with negative pion multiplicity $M_{\pi^-} \geq 2$. Figure 1 shows the negative pion multiplicity distribution. The average observed π^- multiplicity is 9.0 and the average observed charged particle multiplicity is 70. The total number of correlated negative pion pairs (pairs from the same event) is 98 500.

For collisions with unequal target and projectile masses, the dependence of the velocity of the pion emitting source on multiplicity provides useful information about the production process. The number of participants geometrically swept out from the target and the projectile during the collison depends on the impact parameter, and therefore some dependence of the pion source velocity on the pion multiplicity is expected. The velocity of the pion source in the jth event with a given multiplicity M_{π^-} is calculated from

$$\beta_\parallel^{(j)} = \sum_i^{M_{\pi^-}} p_{\parallel i}^{(j)} \Big/ \sum_i^{M_{\pi^-}} E_i^{(j)} \ .$$

In a frame moving with this velocity, the total longitudinal negative pion momentum is equal to zero. The average of $\beta_\parallel^{(j)}$ over all the events of a given pion multiplicity, $\beta_\parallel(M_{\pi^-})$, and the corresponding median value, $\beta_\parallel'(M_{\pi^-})$, are plotted in Fig. 2. The difference between $\beta_\parallel$ and $\beta_\parallel'$ reflects the fact that the distribution of $\beta_\parallel$ for different events with a given multiplicity is skewed. Averaging over all M_{π^-}, we find $\langle\beta_\parallel\rangle = 0.60$ and $\langle\beta_\parallel'\rangle = 0.62$. For comparison, $\beta_\parallel = 0.7$ for the nucleon-nucleon center of mass, and the center of mass frame of the participant nucleons at

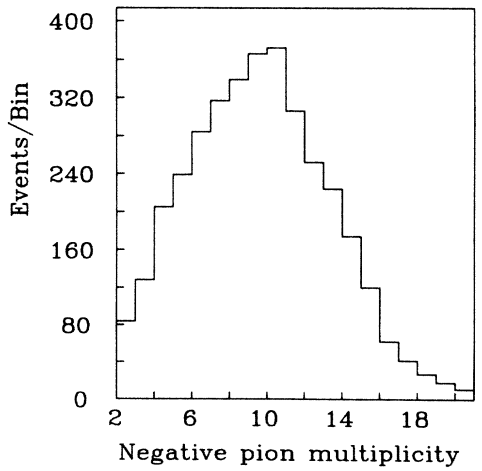

FIG. 1. The negative pion multiplicity distribution for 1.8 GeV/nucleon Ar on Pb.

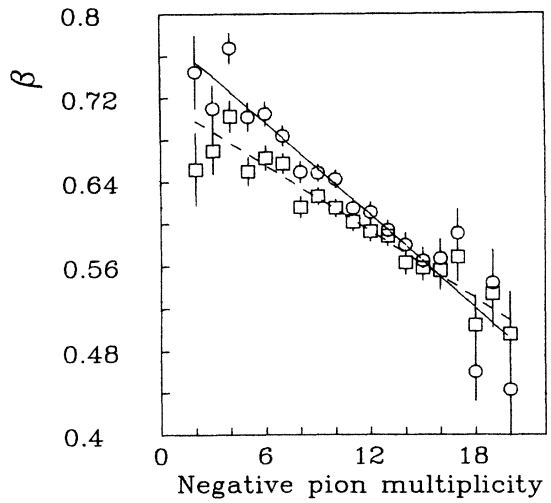

FIG. 2. $\beta_{\parallel}$, the velocity of the pion source, vs M_{π^-}, the negative pion multiplicity. The squares correspond to the average, $\beta_{\parallel}'$. The circles correspond to the median, $\beta_{\parallel}''$.

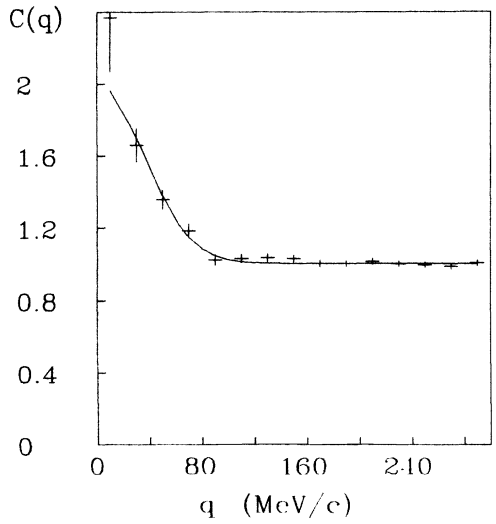

FIG. 3. The data and the fit summed over the relative energy as a function of the relative momentum, q.

zero impact parameter is expected from clean cut geometry to have $\beta_{\parallel}=0.56$.

We have fitted the pion source parameters using both $\beta_{\parallel}$ and $\beta_{\parallel}'$, performing all calculations separately for each multiplicity, and also using both $\langle\beta_{\parallel}\rangle$ and $\langle\beta_{\parallel}'\rangle$. The different values of $\beta_{\parallel}$ change the pion source parameters by less than 5%, which is within measurement errors. In all subsequent interferometry analysis, we choose $\beta_{\parallel}=0.60$. The target absorption for backward pions in the streamer chamber might bias the observed value of $\beta_{\parallel}$. This possible effect can be eliminated by excluding pions with low transverse momentum. The condition $p_t \geq 50$ MeV/c lowers $\beta_{\parallel}$ by less than 1%, and does not affect the pion interferometry analysis. The kinematic selection $p_{\rm lab} \geq 100$ MeV/c has been applied to remove possible electron contamination and reduce the effect of multiple scattering in the target. We estimate that there is still $\sim$3% electron contamination in the data sample after this selection. Monte Carlo simulations indicate that this contamination lowers $\beta_{\parallel}$ by less than 0.6%. Using an event-generating model based on the Vlasov-Uehling-Uhlenbeck equation,[6] we have investigated the possibility that the effective source velocity $\beta_{\parallel}$ might be different for π^-, π^0, and π^+, but have found no noticeable variation.

The linear fits for $\beta_{\parallel}$ and $\beta_{\parallel}'$ show that they both tend to the same value in the high multiplicity limit. It is important to notice that in the limit of large multiplicity (or small impact parameter), both $\beta_{\parallel}$ and $\beta_{\parallel}'$ are at or below the value 0.56, corresponding to the participant velocity at zero impact parameter, assuming clean cut geometry. This suggests that the projectile is completely stopped by the target.

Assuming a Gaussian space-time source,[7] the correlation function takes the form

$$C(q,q_0)=K[1+\lambda\exp(-q^2R^2/2-q_0^2\tau^2/2)] , \quad (1)$$

where q is the relative momentum, q_0 is the relative energy, R is the radius, τ is the lifetime, λ is a measure of the degree of coherence, and K is a normalization factor. The results, after correction for $\pi^- - \pi^-$ Coulomb repulsion by a Gamow factor,[2] are

$$R=5.53\pm0.38 \text{ fm} ,$$
$$\tau=0.0\pm2.5 \text{ fm}/c ,$$
$$\lambda=0.99\pm0.13 .$$

As in previous studies,[3,4] the data are much less sensitive to the lifetime than the radius, which is a consequence of the distribution of $dn/(dqdq_0)$. For the remainder of the analysis, τ will be fixed at 0. The value $\lambda=0.99\pm0.13$ for the degree of coherence is consistent with a totally chaotic source, and a value of $\lambda=0.7$ is obtained without the Gamow factor. As discussed previously,[4] there is a strong correlation between R and λ. The data and the fit, which have been summed over the relative energy, are displayed in Fig. 3.

Next, we take advantage of the relatively large statistics of the present data sample as compared to previous streamer chamber experiments by performing the interferometry analysis with various multiplicity cuts and momentum cuts. In Table I, the results for several multiplicity cuts are listed. The radius in the lowest multiplicity bin, $2\leq M_{\pi^-}\leq 7$, is almost 30% less than that in the other two multiplicity bins. Even if we assume that all the residual Ar on oxygen collisions populate the lowest multiplicity bin, it will account for a reduction in radius of less

TABLE I. Gamow corrected pion source parameters as a function of M_{π^-}, the negative pion multiplicity.

M_{π^-}	π^- pairs	Fit results
$2\leq M_{\pi^-}\leq 7$	9852	$R=3.59\pm0.71$ fm
		$\lambda=0.56\pm0.21$
$8\leq M_{\pi^-}\leq 10$	25 354	$R=5.10\pm0.60$ fm
		$\lambda=1.04\pm0.24$
$11\leq M_{\pi^-}\leq 20$	63 314	$R=5.97\pm0.52$ fm
		$\lambda=1.01\pm0.18$

TABLE II. Gamow corrected pion source parameters as a function of the magnitude of the average momentum of the emitted pion pairs.

$p_{c.m.}$ (MeV/c)	$\langle\|p_1\|+\|p_2\|\rangle/2$	Fit results
$0 \le p_{c.m.} \le 100$	73.5	$R = 6.10 \pm 1.11$ fm
		$\lambda = 0.94 \pm 0.27$
$100 \le p_{c.m.} \le 200$	151.1	$R = 6.12 \pm 0.60$ fm
		$\lambda = 1.34 \pm 0.25$
$200 \le p_{c.m.} \le 300$	246.3	$R = 4.21 \pm 1.21$ fm
		$\lambda = 0.63 \pm 0.29$
$300 \le p_{c.m.} \le 1500$	425.2	$R = 2.99 \pm 0.98$ fm
		$\lambda = 0.97 \pm 0.49$

than 6%. The general trend of the radius increasing with increasing pion multiplicity is consistent with the expectation of a simple geometric picture.

When we perform the interferometry analysis with cuts in the magnitude of the pion momentum, we find a change in the radius of the pion source. In Table II, we list the results of momentum cuts which select pairs in which both pions have momenta within the indicated limits. There is a tendency for the pion source radius to decrease as the average magnitude of the pion momenta increases. In Fig. 4, we display this momentum dependence, taken from Table II. Earlier analysis of 1.5 GeV/nucleon Ar on KCl collisions yielded a similar trend.[4] We have found that the average magnitude of the pion momentum as a function of pion multiplicity is flat within statistical errors, so we conclude that the trends presented in Tables I and II are independent. Monte Carlo simulations show that the pion momentum smearing associated with normal measurement errors depresses the fitted coherence factor by about 15% in the high momentum region, and by a negligible amount elsewhere. Momentum resolution smearing does not distort the source radius in any kinematic region.

The effect of nuclear Coulomb attraction[8] may lower the enhancement of the correlation function in the small q region. Since the final state distribution of nuclear charge may be very complicated, we considered the following three extreme situations. (1) All positive charges remain localized within the volume of the pion source. (2) The Ar and Pb nuclei collide at impact parameter $b = R_{Pb} - R_{Ar}$,

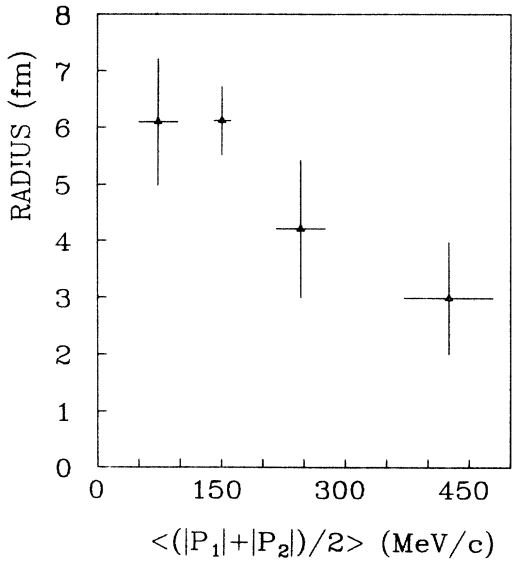

FIG. 4. Radius of the pion emitting source as a function of the average magnitude of the pion pair momenta. This figure does not include the π^--nucleus Coulomb correction which further increases the change in radius.

with the nucleons moving at either participant or target velocity, as prescribed by the clean cut geometric picture. (3) The nuclei collide with zero impact parameter in a clean cut geometric picture. Using the first-order formalism in the classical mechanical limit,[9] we have corrected the momentum of each observed pion in the rest frame of the pion source. We have found that in the worst case, the nuclear Coulomb correction decreases the radius and the coherence factor by 10% and 7%, respectively, for the whole data sample. As expected, the maximum effect on the radius of the nuclear Coulomb correction is larger in the low momentum (< 200 MeV/c) region (14%) than in the high momentum (> 200 MeV/c) region (5%). Therefore, the observed dependence of the pion source radius on the average pion momentum cannot be due to the nuclear Coulomb effect, which tends to suppress this dependence.

Further, we have investigated the spatial shape of the pion source using the following form of the correlation

TABLE III. Pion source shape parameters.

	A. All $p_{c.m.}$	
$R_\parallel = 5.67 \pm 0.54$ fm	For $q_\parallel \simeq 0$	For $q_\perp \simeq 0$
$R_\perp = 5.16 \pm 0.50$ fm	$R_\perp = 5.67 \pm 0.68$ fm	$R_\parallel = 4.13 \pm 0.69$ fm
$\lambda = 0.98 \pm 0.14$	$\lambda = 1.05 \pm 0.22$	$\lambda = 0.78 \pm 0.21$
	B. $0 \le p_{c.m.} \le 200$ MeV/c	
$R_\parallel = 5.99 \pm 0.71$ fm	For $q_\parallel \simeq 0$	For $q_\perp \simeq 0$
$R_\perp = 4.79 \pm 0.62$ fm	$R_\perp = 5.49 \pm 0.72$ fm	$R_\parallel = 5.04 \pm 0.76$ fm
$\lambda = 1.11 \pm 0.20$	$\lambda = 1.20 \pm 0.20$	$\lambda = 1.12 \pm 0.17$
	C. 200 MeV/$c \le p_{c.m.} \le 1500$ MeV/c	
$R_\parallel = 3.26 \pm 0.69$ fm	For $q_\parallel \simeq 0$	For $q_\perp \simeq 0$
$R_\perp = 2.33 \pm 0.40$ fm	$R_\perp = 3.18 \pm 1.43$ fm	$R_\parallel = 1.99 \pm 0.52$ fm
$\lambda = 0.45 \pm 0.11$	$\lambda = 0.64 \pm 0.19$	$\lambda = 0.59 \pm 0.15$

TABLE IV. Pion source parameters with cuts in the quantity $K = |\mathbf{p}_1 + \mathbf{p}_2|/2$.

K (MeV/c)	$\langle K \rangle$ (MeV/c)	Fit results	
$0 \le K \le 150$	101.8	$R = 5.69 \pm 0.57$ fm	$R_\parallel = 6.63 \pm 0.90$ fm
		$\lambda = 0.96 \pm 0.18$	$R_\perp = 5.37 \pm 0.74$ fm
			$\lambda = 1.03 \pm 0.21$
$150 \le K \le 250$	193.8	$R = 5.69 \pm 0.60$ fm	$R_\parallel = 5.88 \pm 0.75$ fm
		$\lambda = 1.28 \pm 0.27$	$R_\perp = 6.23 \pm 0.82$ fm
			$\lambda = 1.31 \pm 0.30$
$250 \le K \le 1500$	322.9	$R = 3.16 \pm 0.55$ fm	$R_\parallel = 3.10 \pm 0.71$ fm
		$\lambda = 0.68 \pm 0.23$	$R_\perp = 2.41 \pm 0.49$ fm
			$\lambda = 0.49 \pm 0.15$

function[2,4]

$$C(q,q_0) = K[1 + \lambda \exp(-q_\parallel^2 R_\parallel^2/2 - q_\perp^2 R_\perp^2/2 - q_0^2 \tau^2/2)] ,$$

where $R_\parallel$ and $R_\perp$ are the longitudinal and transverse pion source dimensions. The fitted parameters are shown in Table III. For the full data sample, we have obtained $R_\parallel \simeq R_\perp$ and $\lambda \simeq 1$, which suggest that the pion source is spherical and totally chaotic. Tables III.B and III.C show the shape parameters of the pion sources for the lower and the higher energy pions. In order to study the directionality of the degree of coherence,[10] we have also fitted the pion source parameters separately in the parallel and the perpendicular directions relative to the beam, by imposing $q_\parallel \simeq 0$ or $q_\perp \simeq 0$. The results are shown in the second and third columns in Table III. We find that there is no significant deviation from a spherical shape and the degree of coherence does not show any directionality for the source of either the lower or the higher energy pions. The dependence of the radius of the pion source on pion momentum may be described by the following physical picture: The more energetic pions are emitted by a pion source produced with earlier "hard" collisions, while the lower energy pions are emitted from the subsequent expanding "fireball" at a lower temperature.

Recent theoretical analysis of a radially expanding fireball with constant temperature[11] also predicts some dependence of the radius on pion momentum. Table IV shows the fitted pion source parameters with cuts in the magnitude of the vector sum of the two pion momenta instead of cuts in the magnitude of both pion momenta in a pair. In order to distinguish between the two cases, it is crucial to measure the dependence of the temperature on the radius of the pion source. Our data show that the c.m. energy distribution for the emitted pions at $\theta_{\text{c.m.}} = 90°$ is not well described by a single exponential, which suggests that the low and the high momentum pions may come from sources at different effective temperatures. The statistics of the data, however, are not enough to give a definitive conclusion.

We conclude that a detailed study of the space-time structure of the pion source in relativistic heavy ion collisions can be made through multiplicity and pion momentum cuts. Our data for central collisions of 1.8 GeV/ nucleon Ar on Pb are consistent with an expanding pion emitting source and are also consistent with a spherical source shape. For collisions of a mass asymmetric system, the dependence of the pion source velocity on multiplicity provides information about the collision dynamics; we find evidence that the Ar nucleus is completely stopped by the Pb target in the most central collisions.

We thank F. Lothrop, J. Brannigan, and the Bevalac staff for their invaluable cooperation. This work is supported by the U.S. Department of Energy.

*Present address: Brookhaven National Laboratory, Upton, NY 11973.

[1] R. Hanbury-Brown and R. Q. Twiss, Nature **177**, 27 (1956); **178**, 1046 (1956).

[2] M. Gyulassy, S. K. Kauffmann, and L. W. Wilson, Phys. Rev. C **20**, 2267 (1979).

[3] S. Y. Fung *et al.*, Phys. Rev. Lett. **41**, 1592 (1978).

[4] D. Beavis *et al.*, Phys. Rev. C **27**, 910 (1983); **28**, 2562 (1983).

[5] W. A. Zajc, Lawrence Berkeley Laboratory Report No. 14864, 1982.

[6] H. Kruse, B. V. Jacak, and H. Stöcker, Phys. Rev. Lett. **54**, 289 (1985); H. Kruse, B. V. Jacak, J. J. Molitoris, G. D. Westfall, and H. Stöcker, Phys. Rev. C **31**, 1770 (1985).

[7] F. B. Yano and S. E. Koonin, Phys. Lett. **78B**, 556 (1978).

[8] W. A. Zajc *et al.*, Phys. Rev. C **29**, 2173 (1984).

[9] M. Gyulassy and S. K. Kauffmann, Nucl. Phys. **A362**, 503 (1981).

[10] G. N. Fowler and R. M. Weiner, Phys. Rev. Lett. **55**, 1373 (1985).

[11] S. Pratt, Phys. Rev. Lett. **53**, 1219 (1984).